Periodica Polytechnica
Civil Engineering

OnlineFirst (2018) paper 10920
https://doi.org/10.3311/PPci.10920
Creative Commons Attribution

Performance-Based Seismic Design and Parametric Assessment of Linked Column Frame System

Shahrokh Shoeibi[1*], Mohammad Ali Kafi[1], and Majid Gholhaki[1]

RESEARCH ARTICLE

Received 21 April 2017; Revised 05 October 2017; Accepted 14 December 2017

Abstract

Linked column frame system, as a new seismic load-resisting system, has a proper seismic behavior in various performance objectives due to ductile behavior of replaceable link beams. Thus, returning to occupancy after moderate earthquake is rapid and low-cost. Performance-based seismic design methods should be used for this system in order to have proper seismic behavior. In this study, by using performance-based plastic design method, a highly accurate and simple design procedure is proposed for this system. 9 prototype structures with 3, 6 or 9 stories and with 3, 4 or 5 bays are selected for parametric design and assessment. For assessment of the designed structures, nonlinear static and dynamic analyses with models according to experimental test results of the members and recommended ground motion records of FEMA P695 are used. According to analyses results, the designed structures in three hazard levels meet the performance objectives.

Keywords

performance-based seismic design, performance-based plastic design, linked column frame system, dual system, nonlinear response history analysis

1 Faculty of Civil Engineering
Semnan University, Semnan, Iran.
* Corresponding author, email: sh.shoeibi@semnan.ac.ir

1 Introduction

In seismic load-resisting systems, there are always members which dissipate the seismic energy by inelastic behavior. Residual deformation and damage due to the inelastic behavior in ductile members, necessitates their replacement in order to return the building to occupancy. The time and cost of repairs depend on the number and layout these members in the structure. In conventional seismic load-resisting systems, such as moment resisting frame or braced frame, repairing and returning the building to occupancy is a costly and time-consuming process because of the large number of the damaged members or their role in bearing gravity loads. Therefore, various systems are proposed in order to be repaired easily and return the buildings to occupancy rapidly. Buckling-restrained braces [1–4], self-centering structural systems [5–7] and linked column frame [8] are examples of such systems.

Linked column frame (LCF) is one of the most recently load-resisting systems proposed by Dusicka et al. [8] which uses conventional components to limit the seismic damage to relatively easy replaceable elements. This seismic load-resisting system, which applies the ductile link beam as a fuse member with shear behavior, leads to prevention or reduction of damage in main structural members in all hazard levels. Limiting the damage to the replaceable shear fuse members reduces the time and cost of repairs, and returns the buildings to occupancy rapidly in this system. There are three ideal performance objectives for LCF system; Immediate Occupancy (IO) with elastic behavior in low earthquake event, Rapid Return to occupancy (RR) with inelastic behavior of link beam in moderate earthquake event and Collapse Prevention (CP) with inelastic behavior of link beams and moment beams in very large earthquake event. The hybrid test results [9] show the proper behavior of this system in these three performance objectives.

A code-based seismic design procedure for this system has been introduced by Malakoutian et al. [10]. The design parameters of this system such as response modification factor (R), system overstrength factor (Ω_0) and deflection amplification factor (C_d) are obtained by Malakoutian et al. [11] as well. This is an elastic force-based method, but proposes an equation based

on pushover analysis only to assure the formation of plastic hinges in link beams before flexural beams. Obviously, force-based methods are simple but unable to determine the inelastic response of the structure under seismic loads. Instead, performance-based or displacement-based methods are the best methods for seismic design due to accurately evaluating the inelastic response such as inelastic displacements, ductility, hysteretic energy and structure's damage. Since an ideal LCF system should have a proper behavior in all three performance objectives, the force-based seismic design methods cannot guarantee the desired function of the structure and performance-based seismic design methods should be applied for this purpose.

Several methods are proposed for displacement-based seismic design. Performance-Based Plastic Design (PBPD) is one of the most recent methods of seismic design which is introduced by Goel et al. [12, 13]. This method is based on the energy equilibrium between inelastic displacement of a structure and presumed yield mechanism. Based on PBPD method, Shoeibi et al. [14] proposed a performance-based seismic design method for dual structures with structural fuse. The aforementioned research is for general purposes and does not present all essential design details.

In this study, first a simplified process is proposed for seismic design of LCF systems according to PBPD concept and then a parametric study was conducted to evaluate the ability of the proposed design method to achieve the LCF system performance objectives. In this proposed method, the ability to adjust yield deflection interval between yielded fuses and yielded beams is provided. This method enables designing for three performance levels of Immediate Occupancy (IO), Rapid Return to occupancy (RR) and Collapse Prevention (CP). The RR performance level is related to the function of the fuse member where yielding and inelastic displacement occur only in these elements and the other structure members remain elastic.

In order to evaluate the applicability of the proposed method and assess the LCF system's performance, a parametric study is done in high seismic risk zone. By this method 9 sample structures with 3, 6 or 9 stories and with 3, 4 or 5 bays in a given plan are designed. Effectiveness and robustness of this method is verified by nonlinear static and dynamic analyses. The structure models are analyzed by Opensees program [15] , and the behavior of members and connections are calibrated with experimental results in order to represent the inelastic behavior of the structure more accurately. The ground motion records, which are used in nonlinear dynamic analysis, are related to three hazard levels of 50% probability of exceedance in 50 years (SLE), 10% probability of exceedance in 50 years (DBE) and 2% probability of exceedance in 50 years (MCE).

2 Design concept of the proposed method for LCF system

2.1 Linked Column Frame system (LCF)

Linked column frame system consists of two systems that work in parallel to provide the desired seismic response (Fig. 1a). The main lateral load-resisting system (structural fuse system), which is called linked column (LC), is made up of two closely spaced columns interconnected with replaceable bolted link beams. The secondary structure system is moment resisting frame (MF) which acts as gravity load bearing system in addition to resisting lateral loads. Replaceable link beams of LCF, first provide the initial stiffness of the system, and then dissipate the seismic energy by ductile and inelastic behavior. Yield of these members limits the inelastic displacements and damages of the adjacent moment resisting frame. Link beams with shear behavior demonstrate high performance for this system duo to proper hysteretic energy dissipation behavior.

There are three performance objectives for ideal behavior of LCF system. First: Immediate Occupancy, where all the LC and MF members remain elastic in earthquakes with 50% probability of exceedance in 50 years. Second: Rapid Return to occupancy, where only link beams enter inelastic phase and yield in earthquakes with 10% probability of exceedance in 50 years, while the other structure members remain elastic. Third: Collapse Prevention, where all the link beams in LC system and flexural beams in MF system are allowed to enter inelastic phase in earthquakes with 2% probability of exceedance in

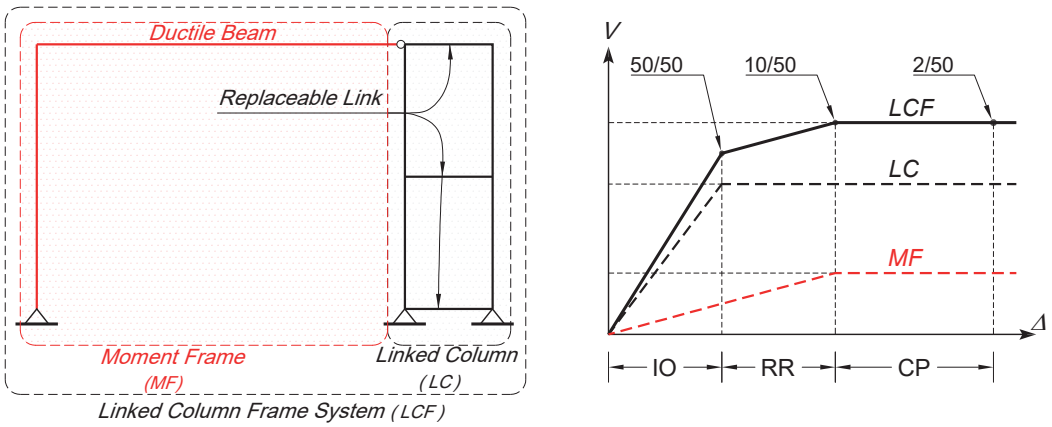

(a) (b)

Fig. 1 (a) Schematic of linked column frame system; (b) Performance objectives of LCF system

50 years. As seen in Fig. 1b, the lateral load capacity curve of LCF system is obtained from summation of capacity curves of linked column system (LC) and moment frame system (MF) which are the base shear curve versus roof displacement. Also, the three performance objective points on the capacity curve are illustrated in this Figure.

2.2 Interactions between LC and MF systems and shear distribution among floors

LCF system has two distinct structure systems with different behaviors which operate together as a dual system. The schematic of these two systems are displayed in Fig. 2a. Lateral displacement of LC system is flexural form, while MF system's lateral displacement is shear form and the dual system has a combination of shear and flexural displacement. These different behaviors cause an interaction between two systems and therefore, the seismic shear story force in each system would be different. It is observed that, in lower floors, LC system has a larger contribution of the shear force, while in upper floors, it has a smaller contribution. The story shear force of MF system in lower floors could be negative or zero which is likely when the relative stiffness of LC system is too high.

In this method, after calculating the base shear for the dual system, the two systems are separated and designed separately. The two systems must be separated in a way to demonstrate their actual behavior in the dual system and preserve the interactive effect between them. The schematic of LCF system under earthquake lateral load of each floor (F_i) is displayed in Fig. 2b. The lateral force must be distributed between the two systems according to their interactions in order to separate the two systems properly. The interactive story shear force is simply calculated by finding the difference between shear story forces for each system. Thus, by elastic analysis of LCF system and determining the story shear loads of each system, the distribution of the lateral load between the two systems of LC and MF is obtained according to their actual interactions (F_i^f, F_i^m). By distributing the lateral load with this method, the two systems could be separated while maintaining their behavior as in the LCF system. Moreover, the story displacements of each system for corresponding lateral loading would be equal to each other and to the LCF system. Separating the capacity curves of two systems is only valid and reliable when executed in this way.

Determining the interaction between the two systems of LC and MF with above method is only valid within the elastic behavior, and by the start of yielding in link beams, the interaction between two systems and the distribution of lateral load would change. In the proposed method, the design of shear link beams and their stiffness proportions are determined in a way that they yield within the limited range of a certain displacement. Hence, the capacity curve of the structure is almost similar to elastic-perfect plastic behavior, and the structure enters the inelastic phase almost instantly. Besides, the proposed equations for separating and considering the interactive effects, are based on the yield point of the LC system, and therefore, this method is independent from the interaction changes in the inelastic phase.

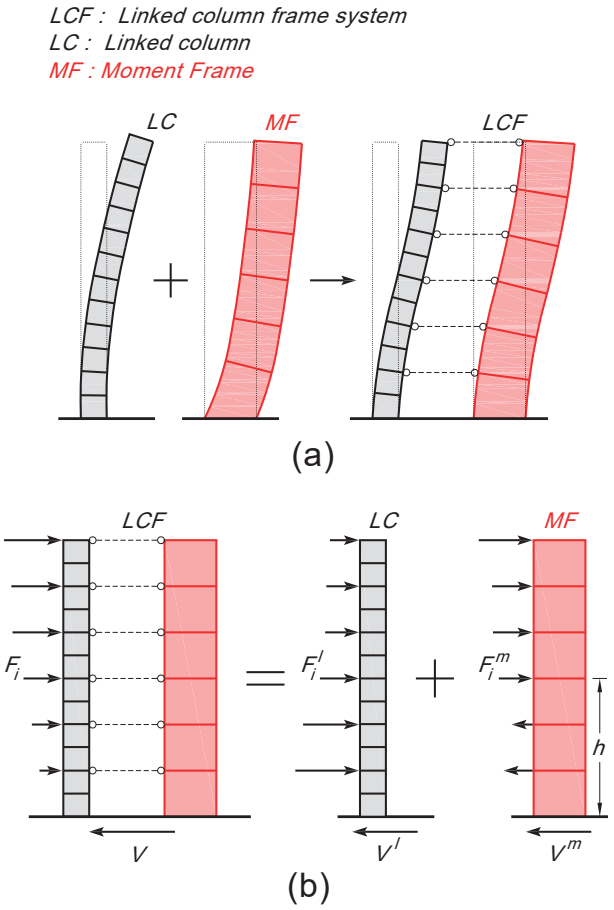

Fig. 2 (a) Schematic of interaction in LCF system; (b) Schematic of separating the LC and MF systems

In this method, the distribution of lateral force is carried out by the equation presented by Chao and Goel [16] as follows:

$$F_i = \lambda_i \tag{1}$$

$$\lambda_i = \left(\beta_i - \beta_{i+1}\right) \ \ when\ i = 1, \beta_{i+1} = 0 \tag{2}$$

$$\beta_i = \left(\frac{\sum_{j=i}^{n} w_j h_j}{w_n h_n} \right)^{aT^{-0.2}} \tag{3}$$

Where, λ_i is the lateral force distribution factor in i^{th} floor, V is the base shear of the LCF system, w_n and w_j are the seismic weights of n^{th} and j^{th} floors respectively, n is the number of structure's stories, h_n and h_j are the elevations of the n^{th} and j^{th} stories respectively, and T is the fundamental period of the structure. The value of is suggested to be equal to 0.5 for LCF system. After analyzing the LCF system and determining the shear loads of both LC and MF systems, the equations below are developed:

$$\lambda_i^l = \frac{F_i^l}{V^l}, \quad \beta_i^l = \frac{V_i^l}{V_n^l}, \quad \beta_i^m = \frac{V_i^m}{V_n^m} \tag{4}$$

Where, λ_i^l is the shear force distribution factor of the LC system, and β_i^l and β_i^m are the shear load ratio of i^{th} floor to the roof in LC and MF systems, respectively. Likewise, V^l is the base shear in LC system, and V_i^l, V_n^l, V_i^m and V_n^m are the shear story of i^{th} and n^{th} floor in LC and MF, respectively.

2.3 General equations of the PBPD method

The basis of the proposed design method of LCF system is the performance-based plastic design. This method, which is introduced by Goel and Chao [12, 13], is based on energy balance for structure's displacement in one direction until reaching the target drift and desired collapse mechanism. This method has been proposed recently for all common structural systems by various researchers because it converges fast and achieves the performance objective of the designer properly [17–20]. In PBPD method, the dissipated elastic energy in an equivalent structure with single degree of freedom is equal to the sum of elastic and plastic internal energy of the structure when it reaches the yield mechanism. The energy balance equation is as follows:

$$E_e + E_p = \gamma E = \gamma \left(\frac{1}{2} M S_v^{\,2} \right) \tag{5}$$

In Eq. (5), E is the input elastic energy, M is the seismic mass of the structure, S_v is the design spectral velocity and γ is the energy modification factor. E_p and E_e are elastic and inelastic energy, respectively, needed for the structure to be pushed up to the target displacement. The relation between the base shear and story drift for the elastic system and elastic-perfect plastic system is displayed in Fig. 3. Having the Eq. (5) and the energy balance in this Figure, γ is calculated as follows:

$$\gamma = \frac{2\mu_s - 1}{R_\mu^2} \tag{6}$$

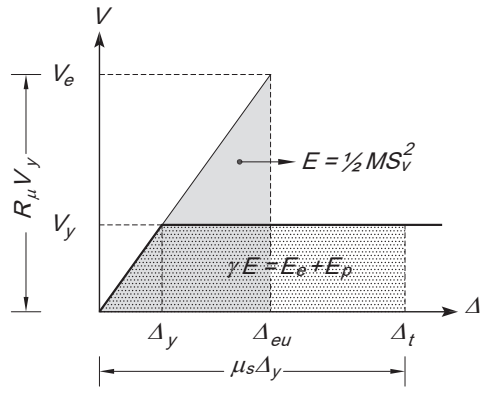

Fig. 3 Idealized response of single degree of freedom structure and the concept of energy balance

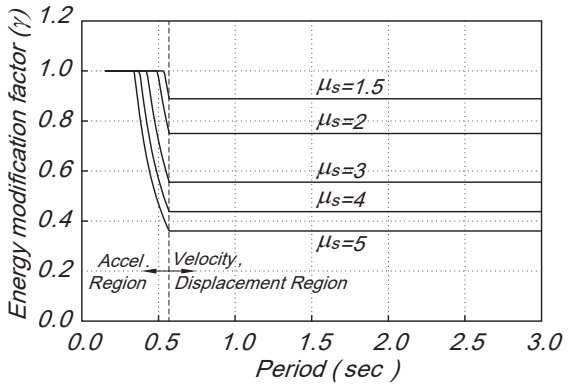

Fig. 4 μ_s, T and γ relations curves

In Eq. (6), μ_s is ductility factor and R_μ is ductility reduction factor which can be calculated by Newmark and Hall [21] equation. The value of γ is derived from the curve in Fig. 4 in relation to the structure's period and ductility factor. By substituting the parameters in energy balance equation, the yield base shear of the structure for achieving the target displacement is calculated as follows:

$$\frac{V_y}{W} = \frac{-\alpha + \sqrt{\alpha^2 + 4\gamma (S_a / g)^2}}{2} \tag{7}$$

$$\alpha = \frac{8\theta_p \pi^2}{T^2 g} \sum_{i=1}^{n} \lambda_i h_i \tag{8}$$

Where, S_a is the spectral acceleration, g is the acceleration of gravity, V_y and W are the yielding base shear and the seismic weight of the structure, respectively and θ_p is the plastic drift ratio which is calculated by yield drift and target drift or the structure's ductility factor. At collapse state, it is assumed that all the stories have a uniform plastic drift ratio and all the plastic deformations are in the same horizontal direction.

2.4 Secondary effects of P-Delta

The secondary effects of P-Delta could cause instability, especially in tall buildings or buildings with inadequate lateral stiffness. In seismic design codes, the necessity of considering this effect and its value according to stability coefficient are presented within the elastic displacements (i.e. ACSE7-10 [22]). In these design codes, since there are limited observations of collapse due to stability, which is because of over strength in the structure, the design elastic drift is used for considering these effects. Previous researches [23] show that considering the elastic displacements does not always lead to realistic results for P-Delta effects. On the other hand, considering inelastic displacements would lead to economically inefficient design. To take an intermediate approach in the proposed method, the yield displacement is chosen for considering the P-Delta effects. However, the nonlinear analysis should be conducted to consider these effects. Therefore, the stability coefficient of the story is defined as follows:

$$SC_i = \frac{\Delta_{y,i}\sum_{j=i}^{n} P_j}{V_{y,i} h_i} = \frac{\sum_{j=i}^{n} P_j}{V_{y,i}}\theta_y \tag{9}$$

Where SC_i is the i^{th} floor's stability coefficient, θ_y is the yield drift ratio, P_j is the j^{th} floor's gravity load, and $V_{y,i}$ and $\Delta_{y,i}$ are the story shear and displacement of the i^{th} floor, respectively, resulted from the yield base shear. If the stability coefficient is lower than 10%, then it is not required to consider the P-Delta effects. Otherwise, the additional base shear (V_a) should be added to the base shear of the structure:

$$V_a = \theta_y \sum_{i=1}^{n} P_i \tag{10}$$

2.5 Separation equations of yield base shear and overturning moment

In Fig. 5, capacity curves of base shear versus roof displacement and overturning moment versus roof drift are displayed. According to this graph, the ratio of elastic base shear and the ratio of elastic overturning moment are defined as $\rho_V = V_e^l / V_e^m$ and $\rho_M = M_e^l / M_e^m$, respectively. V_e^l and M_e^l are elastic base shear and overturning moment in LC system, respectively. Similarly, V_e^m and M_e^m are elastic base shear and overturning moment in MF system, respectively. The yield ratio of the system is defined as $Y_r = \Delta_y^m / \Delta_y^l$ where Δ_y^l and Δ_y^m are the yield displacements in LC and MF systems, respectively. If the yield displacement of MF system happens before the target displacement (Δ_t), considering the bilinear curve, the yield displacement in the structure would be considerably close to the yield displacement of LC system ($\Delta_y \approx \Delta_y^l$). If the yield displacement of structure (Δ_y) is considered exactly equal to that of the MF system, then, $Y_r = \Delta_t / \Delta_y = \mu_s$. Therefore, we would have:

$$\begin{aligned} &V_o^m = \frac{V_y^f}{\rho_V}, \quad V_y^m = Y_r V_o^m, \quad V_y = V_y^f + V_y^m \rightarrow \\ &V_y^f = \frac{V_y}{1 + Y_r / \rho_V}, \quad V_y^m = \frac{V_y}{1 + \rho_V / Y_r} \end{aligned} \tag{11}$$

Similarly, for overturning moment, we would have:

$$M_y^f = \frac{M_y}{1 + Y_r / \rho_M}, \quad M_y^m = \frac{M_y}{1 + \rho_M / Y_r} \tag{12}$$

Because sometimes the base shear of MF system is zero, for calculating the base shear of this system, instead of using the Eq. (11) and distribution on structure's levels, the Eq. (12) is applied.

2.6 Rotational capacity criteria of flexural beams of MF system

In LCF system, the flexural beams should have the adequate rotational capacity to ensure that their yield in MF system happens after the yield of link beams in LC system. Based on classic equation of rotation-moment of a beam with depth of h_b, moment of inertia of I_b, elastic modulus E_s, plastic section modulus of Z_b and length of L_b, we have:

$$\begin{aligned} &M_b = \left(\frac{C_s E_s I_b}{L_b}\right)\theta_b, \quad M_{y,b} = Z_b F_y \rightarrow \\ &\theta_{y,b} = \left(\frac{L_b}{C_s E_s I_b}\right) Z_b F_y = \left(\frac{1}{C_s}\right)\left(\frac{F_y}{E_s}\right)\left(\frac{Z_b}{I_b}\right) L_b, \quad \frac{Z_b}{I_b} \cong \frac{2.2}{h_b} \rightarrow \\ &\theta_{y,b} \cong \left(\frac{1}{C_s}\right)(\varepsilon_y)\left(\frac{2.2}{h_b}\right) L_b = \left(\frac{2.2}{C_s}\right)\varepsilon_y \left(\frac{L_b}{h_b}\right) \end{aligned} \tag{13}$$

Where, $\theta_{y,b}$ is the yield rotational capacity of beam, and C_s is the end support factor which equals 6 for rigid connections at both ends and 3 for rigid connection at one end and pinned connection at the other end. From Eq. (13), it is understood that the rotational capacity of the beam depends on four parameters of its span length, depth, yield stress and end support conditions. As a conservative method, the rotation of beam in each story is considered equal to the story drift, to protect the beams from yielding before the target displacement in RR performance level, the yield rotational capacity of the beams obtained from Eq. (13) must be at least equal to the target drift. When the yield rotational capacity of the beam is lower than

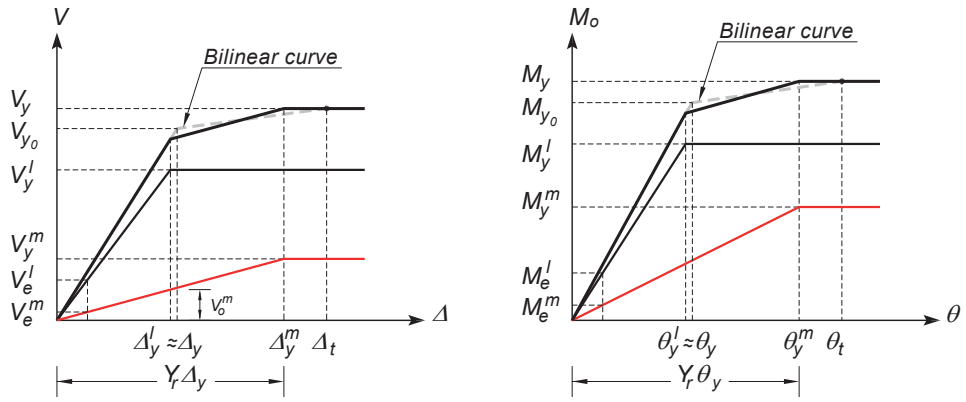

Fig. 5 Capacity curves of base shear versus displacement and overturning moment versus story drift

the target drift, the flexural beams would yield before the target drift, and therefore, Y_r would be calculated approximately from the following equation:

$$Y_r = \Delta_y^m / \Delta_y^l = \theta_y^m / \theta_y^l \cong \theta_{y,b} / \theta_y^l \tag{14}$$

2.7 Design of ductile members of LC system

In LC system, because the shear force of each story corresponds to the shear ratio (β_i^l) of it, the shear ratio of link beams of each story ($\bar{\beta}_i^l$) is calculated from portal frame analysis as follows:

$$\bar{\beta}_i^l = \begin{cases} 1 & i = n \\ \beta_i^l + \beta_{i+1}^l & i \neq n \end{cases} \tag{15}$$

In Fig. 6a, an LC frame with shear link beam as fuse is illustrated where the desired mechanism is the shear yield of link beams. If the shear force of roof's link beam is equal to V_r, the value of shear force in i_{th} floor's link beam would be $\bar{\beta}_i^l V_r$. Analysis results show that the shear forces of the mid-story link beams and above the base link beam are approximately equal to $\bar{\beta}_i^l V_r$ and $1.5\,\bar{\beta}_i^l V_r$, respectively. And according to the balance of internal and external virtual work equation, V_r is calculated as follows:

$$\begin{gathered} \sum_1^n F_i^l \Delta_i = \sum_0^n V_{l,i} \left(\gamma_p e_c\right) \rightarrow \\ \sum_1^n F_i^l h_i \theta_p = \theta_p e \sum_0^n V_{l,i} \\ \gamma_p = \theta_p e / e_c, \quad V_{l,i} = 2.5 \bar{\beta}_i^l V_r \rightarrow \\ \sum_1^n F_i^l h_i = e\left(\sum_1^n 2.5 \bar{\beta}_i^l V_r + \bar{\beta}_1^l V_r\right) \rightarrow \\ V_r = \frac{\sum_1^n F_i^l h_i}{e\left(\sum_1^n 2.5 \bar{\beta}_i^l + \bar{\beta}_1^l\right)} \end{gathered} \tag{16}$$

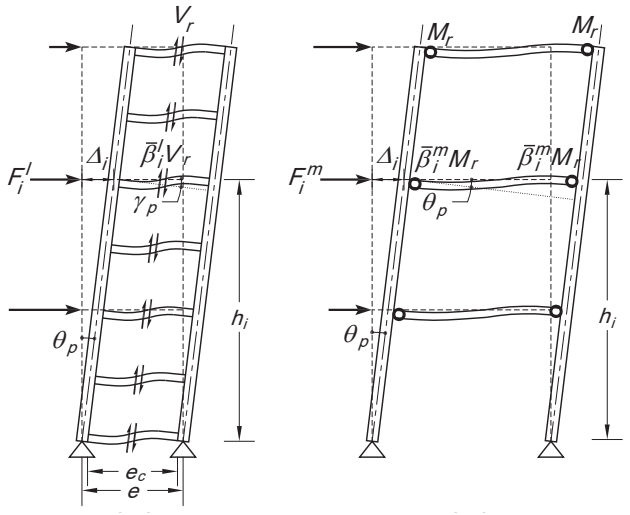

(a) (b)

Fig. 6 (a) Yield mechanism in LC system; (b) Yield mechanism in MF system

Having calculated the value of V_r, the shear forces of all link beams of LC system are obtained. In design of the link beams, they assumed to have a shear behavior, and therefore, according to the provisions of the ASCE 341-10 [24] for the link beams of the eccentrically braced frames, the equation $e_c \leq 1.6 M_p / V_p$ must be satisfied for the link beam's section. Where A_w is the shear cross sectional area of the beam, and yield stresses in the beam's web and flange are identical, the criteria for shear behavior would be as follows:

$$Z_b \geq 0.375 A_w e_c \tag{17}$$

2.8 Design of ductile members of MF system

Title in Fig. 6b, the MF system with yielding flexural beams and the yield mechanism of moment connection at the end of beam are displayed. In this system, the shear force of each story corresponds to the shear ratio (β_i^m) of it, and the bending moment ratio of beams of each story ($\bar{\beta}_i^m$) is approximately calculated by portal frame analysis as follows:

$$\bar{\beta}_i^m = \begin{cases} 1 & i = n \\ \beta_i^m + \beta_{i+1}^m & i \neq 1, n \\ 2\beta_1^m + \beta_2^m & i = 1 \end{cases} \tag{18}$$

If the bending moment of roof's beam is equal to M_r, the value of bending moment in i^{th} floor's beam would be $\bar{\beta}_i^m M_r$. Then the virtual work balance could be used. But because sometimes the base shear of MF system is zero, or nearly zero, the distribution of lateral force cannot be carried out according to the base shear. Thus, in virtual work balance equation of these systems, the overturning moment is used for determining M_r as follows:

$$\begin{gathered} \sum_1^n F_i^m \Delta_i = \sum M_{b,i} \theta_p \\ \sum_1^n F_i^m \Delta_i = \theta_p \sum_1^n F_i^m h_i = \theta_p M_y^m \\ M_{b,i} = \bar{\beta}_i^m M_r \rightarrow \\ \theta_p \sum_1^n M_y^m = \theta_p \sum_1^n M_{b,i} \rightarrow \\ M_r = \frac{M_y^m}{\sum_i^n n_r \bar{\beta}_i^m} \end{gathered} \tag{19}$$

Where, n_r is the number of yielding points in each story and $M_{b,i}$ is the moment of the i_{th} floor's beam.

Based on M_r value, the bending moments of the flexural beams of the MF system could be calculated. These beams should be designed in a way to satisfy the required yield rotational capacity in RR performance level. Where various bay lengths or beam stiffness exist in the structure, the M_r calculated from Eq. (19) is the average bending moment of the roof, and the end moment of each beam would be calculated according to its flexural stiffness from the total bending moment of the roof ($M_r n_r$).

3 The proposed procedure of design for LCF system

The proposed design method for LCF systems is an iterative approach to reach a convergence point because the two systems need to be designed separately while considering their interactions. The yield mechanism for LCF systems, in both RR and CP performance levels, are the shear yield of link beams in LC system and flexural yield of ductile beams in MF system at the target displacement. The design steps of the proposed method are as follows:

1. Determining the target drift (θ_t) for the hazard levels in performance levels of RR and CP. Determining the gravity loads and structure's mass according to design code (i.e. [22] or [25]).
2. Calculating the fundamental period of the structure. For this purpose, a structure with pre-assumed stiffness could be analyzed.
3. Distribution of lateral loads on LCF structure according to Equations 1–3.
4. Calculating the interactions and shear forces of the LC and MF systems according to elastic analysis of LCF structure. Distribution of lateral load for both LC and MF systems, and calculating the parameters of λ_i^l, β_i^l and β_i^m according to Equations 4.
5. Calculating the plastic drift (θ_p) for two performance levels of RR and CP from equation: $\theta_p = \theta_t - \theta_y$. For LCF system, the yield drift (θ_y) value of 1% is suitable. Calculating γ from Eq. (6) and μ_s from: $\mu_s = \theta_t / \theta_y$.
6. Calculating yield base shear of LCF system from Equations 7–8 for two performance levels of RR and CP ($V_{y,RR}$ and $V_{y,CP}$). $V_{y,RR}$ and $V_{y,CP}$ are calculated by design spectrums of DBE and MCE, respectively.
7. Calculating the yield base shear of LCF system in performance level of IO ($V_{y,IO}$) by design spectrum of SLE and from the equation: $V_{y,IO} = S_{a,SLE}W$. Where $S_{a,SLE}$ is the spectral acceleration related to SLE design spectrum.
8. Determining the yield shear of LCF system (V_y) which is the maximum of $V_{y,RR}$, $V_{y,CP}$ and $V_{y,IO}$.
9. Controlling the stability coefficients of the stories from Eq. (9), and calculating the additional base shear from Eq. (10) if necessary.
10. Determining the value of Y_r by calculating the minimum capacity of yield drift ratio of beams according to the parameters of span length, depth, yield stress and end support conditions of the beams.
11. Calculating base shear of LC system from Eq. (11), and designing its link beams according to base shear (V_y^l), lateral force distribution factor (λ_i^l), shear load ratio of story (β_i^l), shear force ratio of beam ($\bar{\beta}_i^l$) and Eq. (17). For design of these members, the general provisions of seismic design (i.e. AISC 341-10 [24]) should be considered.
12. Calculating the yield overturning moment of MF system from Eq. (12), and designing its flexural beams according to yield overturning moment (M_y^m), shear load ratio of story (β_i^m) and bending moment ratio of beam ($\bar{\beta}_i^m$). For design of these members, the general provisions of seismic design (i.e. AISC 341-10 [24]) should be considered.
13. Designing the columns of LCF system according to the shear yield of link beams and flexural yield of ductile beams with considering the factors of $1.25R_y$, where R_y is the ratio of the expected yield stress to the specified minimum yield. In design process of columns, seismic design provisions [24] such as strong column/weak beam and strength of panel zone should be considered too.
14. Controlling the convergence of the design according to the fundamental period of the structure or the yield base shear. When the convergence is not achieved, return to step 2.
15. If the convergence is achieved, the final design of LCF system should be checked by nonlinear static or dynamic analysis.

4 Application of the proposed method for designing a structure with linked column frame system

4.1 Prototype structures

To design the LCF system with the proposed method, the floor plan of a building with dimensions of 25m × 25m is used as displayed in Fig. 7. The structures have 3, 6 or 9 stories with story height of 3.80 meters and the number of bays in MF system is 3, 4 or 5 with equal lengths. Generally, there are 9 different structures to be designed by the proposed method. The lateral load resisting system is placed on the perimeter of the building, and the internal beams and columns only resist the gravity loads. In perimeter of the building, there is one bay of ductile link beam which has the span lengths (e) of 1.2, 1.6 and 2 meters for 3-story, 6-story and 9-story buildings, respectively. The dead and live loads of the floors are assumed 5.5 kN/m^2 and 3 kN/m^2, respectively, and roof's dead and live loads are assumed as 6.5 kN/m^2 and 1.5 kN/m^2, respectively. Weights of external walls and roof's parapet are assumed 6.4 kN/m and 2 kN/m, respectively. Therefore, the seismic masses of the floors and the roof are calculated as 453.9 ton and 516.6 ton, respectively.

The design spectrums are according to Iran's Standard No. 2800 [25] and based on this code, the buildings are located in very high seismic risk zone and on soil type II. The design spectrum for the earthquake with 10% probability of exceedance in 50 years (DBE) is assumed according to this design code. The design spectrum for the earthquake with 2% probability of exceedance in 50 years (MCE) is considered as 1.5 times of the design spectrum for DBE which is displayed in Fig. 9. According to this, the spectral acceleration at short period for DBE and MCE are calculated as 0.875g and 1.312g, respectively. The design spectrum for the earthquake with 50% probability of exceedance in 50 years (SLE) is according to Fig. 9, and the spectral acceleration at short period is

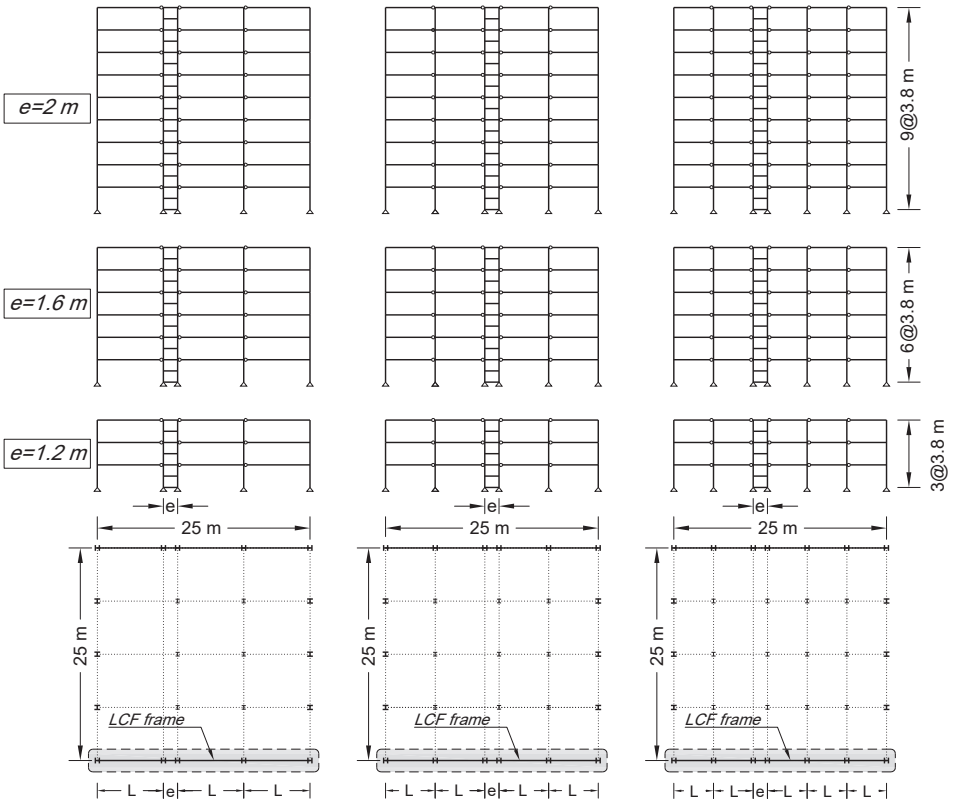

Fig. 7 Floor plan of prototype structure and elevation view of the 3-, 6- and 9-story frames

Table 1 Design parameters used for LCF design in three performance objectives

Performance Level	Parameter	S-313	S-314	S-315	S-613	S-614	S-615	S-913	S-914	S-915
	Iterate #	2	2	3	2	2	2	3	2	2
	W (kN)	6,987	6,987	6,987	13,666	13,666	13,666	20,345	20,345	20,345
	T (s)	1.117	1.096	1.104	1.930	1.927	1.826	2.525	2.627	2.36
	SC_1	0.072	0.072	0.072	0.109	0.109	0.110	0.135	0.133	0.137
	V_a	0	0	0	176	176	176	263	263	263
Rapid Repair										
	θ_t	0.02	0.02	0.02	0.02	0.02	0.02	0.02	0.02	0.02
	θ_y	0.01	0.01	0.01	0.01	0.01	0.01	0.01	0.01	0.01
	θ_p	0.01	0.01	0.01	0.01	0.01	0.01	0.01	0.01	0.01
	μ_s	2	2	2	2	2	2	2	2	2
	R_μ	2	2	2	2	2	2	2	2	2
	γ	0.75	0.75	0.75	0.75	0.75	0.75	0.75	0.75	0.75
	S_a/g	0.440	0.447	0.444	0.292	0.292	0.303	0.243	0.237	0.254
	α	0.650	0.676	0.666	0.423	0.424	0.472	0.367	0.340	0.420
	V_y (kN)	1,227	1,228	1,227	1,611	1,610	1,600	1,952	1,970	1,921
Collapse Prevention										
	θ_t	0.03	0.03	0.03	0.03	0.03	0.03	0.03	0.03	0.03
	θ_y	0.01	0.01	0.01	0.01	0.01	0.01	0.01	0.01	0.01
	θ_p	0.02	0.02	0.02	0.02	0.02	0.02	0.02	0.02	0.02
	μ_s	3	3	3	3	3	3	3	3	3
	R_μ	3	3	3	3	3	3	3	3	3
	γ	0.556	0.556	0.556	0.556	0.556	0.556	0.556	0.556	0.556
	S_a/g	0.660	0.670	0.666	0.437	0.438	0.455	0.365	0.356	0.382
	α	1.300	1.353	1.333	0.846	0.848	0.943	0.734	0.679	0.839
	V_y (kN)	1,153	1,150	1,151	1,517	1,516	1,491	1,829	1,860	1,776
Immediate Occupancy										
	S_a/g	0.160	0.62	0.161	0.106	0.106	0.110	0.088	0.086	0.092
	V_y (kN)	1,115	1,133	1,126	1,446	1,448	1,504	1,798	1,753	1,879

Table 2 Period and the design forces of LCF, LC and MF systems in design iterations

Frame	Iterate #	T(s)	V_y^{lcf}(kN)	V_y^{l}(kN)	V_y^{m}(kN)	V_r(kN)	M_r(kN-m)	M_y(kN-m)	M_y^{l}(kN-m)	M_y^{m}(kN-m)	T_{new}(s)	Diff. (%)
S-313												
	1	**0.908**	1322	1043	280	185	604	13275	6847	6427	**1.117**	23.0
	2	**1.117**	1227	1317	-89	280	525	12383	9217	3167	**1.045**	6.40
S-314												
	1	**0.802**	1467	959	507	121	537	14683	5731	8952	**1.096**	36.7
	2	**1.096**	1228	1271	-43	238	414	12386	8189	4197	**1.088**	0.70
S-315												
	1	**0.698**	1833	1015	818	85	551	18294	5602	12692	**0.982**	40.7
	2	**0.982**	1238	1146	92	187	343	12459	6681	5778	**1.104**	12.4
	3	**1.104**	1228	1336	-108	292	305	12385	9036	3349	**1.058**	4.20
S-613												
	1	**1.754**	1767	1461	306	-5	870	34481	14350	20132	**1.93**	10.0
	2	**1.930**	1786	1854	-68	97	789	34959	20287	14672	**1.842**	4.60
S-614												
	1	**1.497**	1915	1323	592	-25	684	37208	11571	25637	**1.927**	28.7
	2	**1.927**	1785	1810	-25	98	568	34953	18067	16886	**1.852**	3.90
S-615												
	1	**1.281**	1959	1156	803	-21	528	37888	9275	28613	**1.826**	42.5
	2	**1.826**	1775	1638	137	89	434	34690	14713	19978	**1.827**	0.10
S-913												
	1	**2.595**	2228	1857	372	-73	1102	64841	24131	40712	**2.692**	3.7
	2	**2.692**	2244	2321	-77	33	971	65370	35071	30299	**2.525**	6.2
	3	**2.525**	2216	2397	-181	59	941	64433	39785	24648	**2.494**	1.20
S-914												
	1	**2.183**	2241	1575	666	-60	765	64888	18309	46580	**2.627**	20.3
	2	**2.627**	2234	2252	-20	56	658	65021	30260	34760	**2.496**	5.00
S-915												
	1	**1.851**	2480	1499	981	-40	616	71450	16180	55271	**2.360**	27.5
	2	**2.360**	2184	2026	159	64	472	63382	23749	39633	**2.419**	2.50

calculated as 0.419g. The link beams of the LC system have the shear behavior, and the moment resisting beams of the MF system have flexural behavior. The connection of the columns to the foundation is pinned. In MF system, to increase the rotational capacity of the flexural beams, their connection at one end is pinned as well. To increase the load resisting capacity of the system, link beams are also used in mid-story and above the base. The floor loads are carried in north-south direction. The prototype name is combination of number of stories, number of LC system and then number of bays.

4.2 Designing the prototype structures

For design of this structure against DBE earthquake and for performance level of RR, the target drift is assumed as 2%. The target value for the performance level of CP against the MCE earthquake is 3%. The type of steel material is A992 with yield stress of 345 MPa. As the initial guess to start the iterative design process, the stiffness of beams and columns are assumed equal. To calculate the fundamental period of structure and shear forces of the stories, modeling and elastic analysis are carried out by computer software. The design parameters of the last iteration of the design process for 9 prototype structures in 3 performance objectives are presented in Table 1. It is seen in the table that the stability coefficient of the first floor for all 3-story structures are lower than 10%, and therefore, the additional base shear resulted from P-Delta effects (V_a) is zero. However, in 6- and 9-story prototypes, the additional base shear (V_a) is added to design base shear because the stability coefficient is higher than 10%.

As observed from Table 2, the iterations of the design procedure for all prototypes. These numbers of iterations are based on identical sections for all members as initial guess, and they would be improved with a more proper initial guess. However, as seen in the table, the maximum number of iterations is three times only. The convergence criterion for the design is the period of the structure with maximum 5% error. The yield base shear and corresponding overturning moment of the whole structure and contribution of LC and MF systems in these factors are shown in this table. The roof design shear force of link beam (V_r) and roof design bending moment of ductile beam (M_r) are also presented in Table 2.

Table 3 The designed sections of the members in S-615 and S-915 structures

Frame	Story	Linked column system			Moment frame system		
		Story link	Mid-story Link	Column	Exterior column	Interior column	Beam
S-614							
	6	I30×1-20×2	I30×1-20×2	W14×61	W14×68	W14×99	W10×88
	5	I30×1-20×2	I30×1-20×2	W14×90	W14×68	W14×99	W12×136
	4	I30×1-20×2	I32.5×1-20×2	W14×132	W14×90	W14×109	W12×152
	3	I30×1-20×2	I42.5×1-17.5×2	W14×159	W14×90	W14×132	W12×136
	2	I40×1-17.5×2	I55×1-17.5×2	W14×211	W14×90	W14×132	W12×136
	1	I57.5×1.2-17.5×2	I65×1.5-22.5×2	W14×370	W14×90	W14×132	W10×100
S-914							
	9	I30×1-27.5×2	I30×1-27.5×2	W14×74	W14×82	W14×120	W12×136
	8	I30×1-27.5×2	I30×1-27.5×2	W14×99	W14×90	W14×132	W12×190
	7	I30×1-27.5×2	I30×1-27.5×2	W14×120	W14×99	W14×145	W12×230
	6	I30×1-27.5×2	I35×1-25×2	W14×159	W14×120	W14×159	W12×230
	5	I30×1-25×2	I42.5×1-25×2	W14×211	W14×120	W14×176	W12×230
	4	I37.5×1-25×2	I50×1-25×2	W14×257	W14×120	W14×176	W12×230
	3	I47.5×1-25×2	I55×1.2-27.5×2	W14×311	W14×120	W14×176	W12×190
	2	I50×1.2-27.5×2	I67.5×1.2-25×2	W14×398	W14×120	W14×176	W12×152
	1	I70×1.2-25×2	I77.5×1.5-22.5×2.5	W14×550	W14×120	W14×176	W12×96

The link beams are built-up sections, and W-sections are used for the columns and flexural beams. Another rule for column design is that the column sections could not be weaker than the above floors columns. In Table 3, the designed sections of members of two structures (S-615 and S-914) are presented as examples. In this table, the dimensions for built-up sections of link beams are in centimeters and indicate the dimensions of web and flange, respectively. As observed from this table, because of the interactions between two systems in the height of the structure, link beam sections in lower stories are bigger than the upper stories, and the flexural beam sections in upper stories are bigger than the lower stories.

5 Evaluating the performance of LCF system designed with the proposed method

To evaluate the buildings designed by this method for three performance objectives, the structures are modeled accurately, and nonlinear static and dynamic analyses are performed on them. For nonlinear dynamic analysis, the ground motion records recommended by FEMA P695 [26] are used. These analyses are carried out by Opensees program [15].

5.1 Structure modeling

The structure members are modeled as beam-column elements and the rigid end offsets are considered in their modeling. All members have fiber cross sections, and material behaviors of link and flexural beams are calibrated by experimental force-displacement hysteretic loops.

Because of using link beams with ductile shear behavior, material properties of these elements are calibrated with experimental results of Dusicka and Lewis [27]. They have used suggested detailing for the link beams of LCF system in their specimens. In Fig. 8a the hysteretic graph of shear force versus link beam rotation is compared for the experiments of Dusicka and Lewis on shear link beam and the model calibrated for the Opensees. The allocated moment connection for the LCF system is bolted unstiffened extended end-plate connection. Therefore, the material's flexural behavior of the link beams and yielding flexural beams are as their connections, and they are calibrated by the experiments of Sumner and Murray [28]. To consider the degradation effects in flexural behavior model, the fatigue model is combined with the flexural model. In Fig. 8b, the moment-plastic rotation curve of Sumner and Murray experiment along with the analytical model of Opensees are displayed. To model the behavior of the columns of the structure, the existing model of Steel02 in the software is used. In modeling of all members in Opensees, the shear and flexural behaviors are aggregated to consider the effects of the shear deformations in the analysis properly. All the pinned connections are calibrated with behavior models of experiments of Liu and Astaneh [29] to consider the slight moment stiffness of these connections in analysis. Because the seismic design provisions are considered in the design process, and the capacity of the panel zone is accounted for, the shear deformation of the panel zone and its effect on the analysis is negligible. Therefore, panel zone is not considered in the modeling. To have a more realistic model, and to have the actual length of the link beam, rigid end offsets are considered in the model. Floors are considered to be rigid diaphragms in the models.

P-Delta effects are considered in the modeling. For this purpose, the gravity loads on the frame are applied on their actual locations and the rest of gravity loads are applied to the P-Delta leaning column.

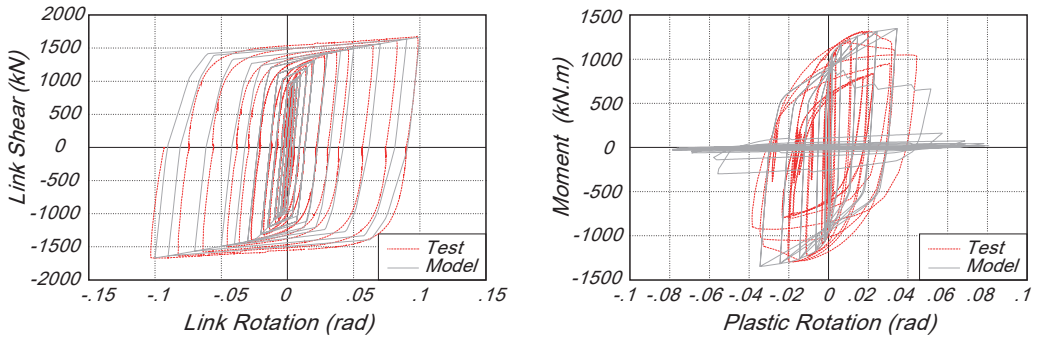

(a) (b)

Fig. 8 (a) Comparison between Opensees model and the experiment of Dusicka and Lewis [27] for the link beam; (b) Comparison between Opensees model and the experiment of Sumner and Murray [28] for the moment connections

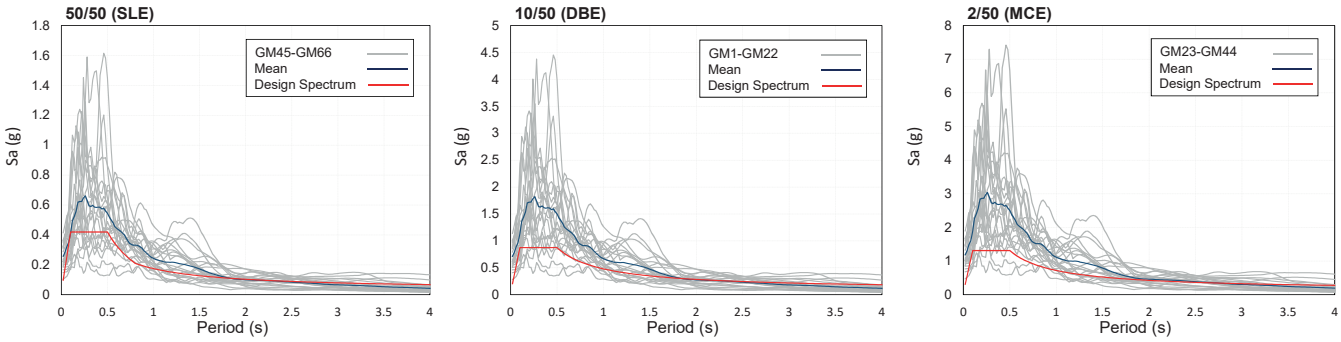

Fig. 9 The design and scaled response spectrums in three hazard levels

5.2 Selected ground motion records

For nonlinear dynamic analysis, the recommended ground motion records of FEMA P695 [26] are used. From 22 pairs of ground motion records, 22 records in direction 1 are selected. The selected records are scaled with the design spectrums of three hazard levels of SLE, DBE and MCE obtained from Iran's Standard No. 2800 [25] in periods between 0.3 and 3.15 seconds. The calculated scale factors are 0.69, 1.9 and 3.16 for SLE, DBE and MCE hazard levels, respectively. In Fig. 9, the design spectrum, response spectrum of the scaled ground motion records and the mean of response spectrums in three hazard levels are displayed. The ground motions from GM45 to GM66 belong to SLE hazard level, from GM1 to GM22 belong to DBE hazard level and from GM23 to GM44 belong to MCE hazard level.

5.3 Nonlinear static analysis results

After designing the prototype structures with the proposed method, the accurate models of structures are analyzed. The results of nonlinear static analysis for 9 prototype structures are presented in Table 4. The parameters include yield drift, target drift in three hazard levels, the drift value of first yield in any of link beams of LC system and the drift value of first yield in any of flexural beams of MF system. The value of yield drift and target drift are obtained from pushover capacity curves and by the method described in ASCE 41-13 [30]. As observed in this table, the target drift in SLE hazard level is lower than the drift of first yield point in link beam, which means that the structure members are remained elastic in this

Table 4 The target and yield drift and drift at the first members yielded obtained from pushover analysis

Frame	θ_y(%)	θ_t(%)			$\theta_{y\ 1st\ LC}$ (%)	$\theta_{y\ 1st\ MF}$ (%)	$\theta_{y\ 1st\ MF}/\theta_{y\ 1st\ LC}$
		SLE	DBE	MCE			
S-313	0.87	0.56	1.54	2.30	0.79	2.73	3.46
S-314	0.87	0.57	1.56	2.32	0.79	2.42	3.07
S-315	0.87	0.55	1.51	2.25	0.76	2.85	3.74
S-613	1.21	0.62	1.71	2.50	1.08	2.36	2.18
S-614	1.14	0.63	1.70	2.48	0.98	2.40	2.45
S-615	0.99	0.62	1.68	2.43	0.94	2.09	2.23
S-913	1.44	0.65	1.82	2.63	1.31	2.28	1.74
S-914	1.24	0.66	1.78	2.56	1.10	2.20	2.01
S-915	1.05	0.57	1.70	2.43	0.94	1.78	1.89

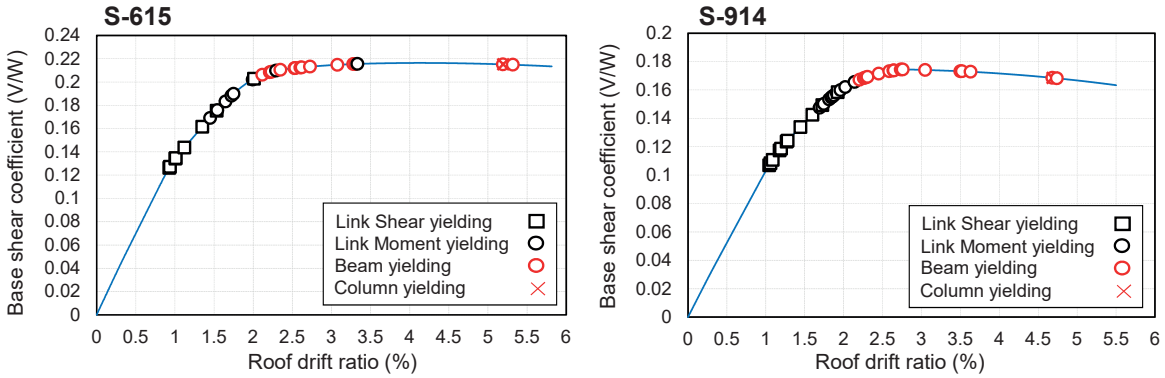

Fig. 10 Pushover capacity curve and yield stages of structure members in S-615 and S-914 prototype structures

hazard level. The maximum target drift in DBE hazard level is 1.82% which is lower than the pre-assumed value of 2%. Similarly, the maximum target drift in MCE hazard level is 2.63% which is lower than the pre-assumed value of 3%. Therefore, the designed structures achieve the desired performance objectives successfully. The yield drift values obtained from pushover analysis are different from the pre-assumed value of 1% in some structures. This value could be corrected in design iterations to achieve a more accurate design.

By comparing the drift of first yield point of link beam in LC system with the drift of first yield point in flexural beam of MF system, it is obvious that yield interval between the two systems is adequate, and therefore, the link beams function efficiently as fuse elements.

The pushover curve and yield points of the ductile members of S-615 and S-914 structures are displayed in Fig. 10 as an example. As observed, first all link beams yield, and then the flexural beams enter the inelastic phase and undergo the permanent deformations. The yield process of members in the structure displays the yield mechanism of the structure as well.

5.4 Nonlinear dynamic analysis results

After designing the prototype structures with the proposed method, the accurate models of the two structures of S-615 and S-914, under scaled ground motion records of three hazard levels, are analyzed by nonlinear dynamic method to evaluate the seismic behavior of the structure comprehensively. The analysis results indicate that the designed structures with the proposed method achieve the desired performance objectives successfully.

5.4.1 Story drifts

In Fig. 11 the maximum story drifts for the earthquake with exceedance probability of 10% and 2% in 50 years (MCE and DBE) are displayed for the two considered prototypes. As observed in these graphs, for the DBE in S-615 structure, the maximum of median story drift is occurred in sixth floor which is 1.84% and its minimum in third floor is 1.62%. In the S-914 structure and in the same hazard level, maximum of median story drift is occurred in seventh floor which is 1.91% and its minimum in first floor is 1.25%. The pre-selected target drift for design in hazard level of DBE is 2%, and the obtained median drift of both structures are lower than the target value. For MCE in S-615 structure, maximum of median story drift is occurred in first floor which is 2.84% and its minimum in sixth floor is 2.29%. In S-914 structure and in the same hazard level, maximum of median story drift is occurred in sixth floor which is 2.58% and its minimum in ninth floor is 2%. The pre-selected target drift for design in hazard level of MCE is 3%, and the obtained median drift of both structures are lower than the target value. As observed in these graphs, the 84th percentile value, which is the median value plus a standard deviation, is exceeded the target value in general. From these graphs, it is understood that the designed structures with the proposed method achieve the desired performance objectives successfully.

5.4.2 The yield of members

To control the yield in structure members, the shear DCR, which is the ratio of maximum shear to the yield shear in the link beam, and the moment DCR, which is the ratio of maximum bending moment to the yield moment in ductile beams, are obtained from the nonlinear dynamic analysis. In Fig. 12, the values of shear DCR of the link beam and moment DCR of the ductile beams for the earthquake with exceedance probability of 50% in 50 years (SLE) for S-615 and S-914 prototypes are presented. According to this Figure, the maximum of median moment DCR of the ductile beam for S-615 and S-914 prototypes are 0.534 and 0.481, respectively, and 100% of the data are lower than 1 in this hazard level. Therefore, no member of MF system is entered the inelastic phase in this hazard level. Similarly, the maximum of median shear DCR of the link beam for S-615 and S-914 prototypes are 1.077 and 1.028, respectively. This means that the shear link beams of LC system are in the yield limit and have not entered the inelastic behavior phase yet. Therefore, in SLE hazard level, all the members have an elastic behavior which is the target for the proposed method.

In Fig. 13, the values of moment DCR of the flexural beams of the MF system for the earthquake with exceedance probability of 10% in 50 years (DBE) for the S-615 and S-914 prototypes are demonstrated. According to this Figure, the maximum of median moment DCR of the yielding beams for S-615

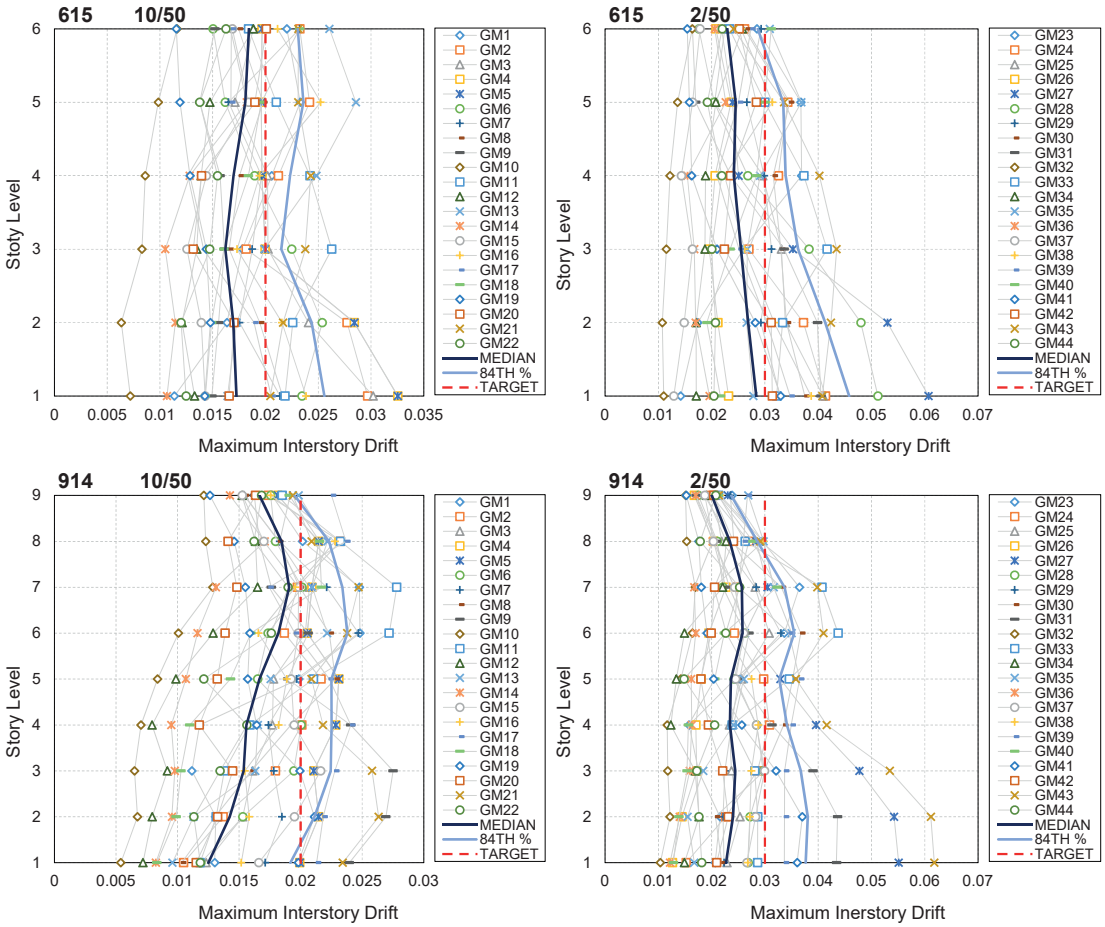

Fig. 11 Maximum story drift in S-615 and S-914 prototype structures for DBE and MCE

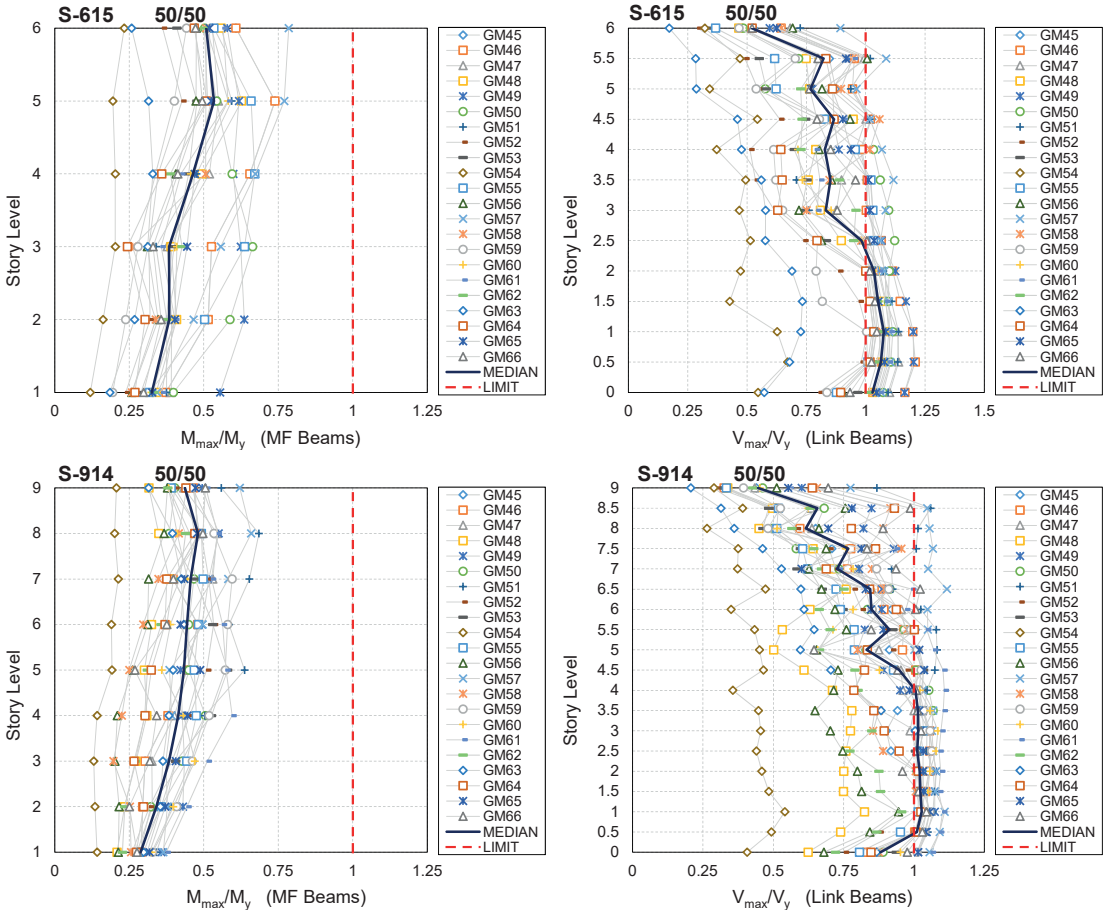

Fig. 12 Shear DCR of link beams and moment DCR of flexural beams in S-615 and S-914 prototype structures for SLE hazard level

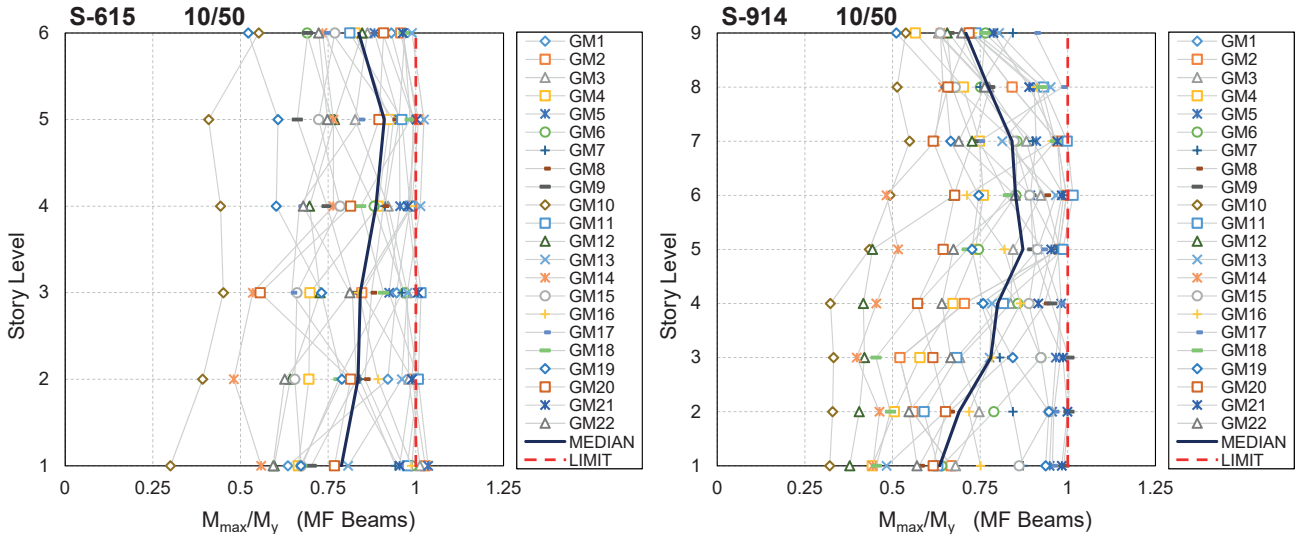

Fig. 13 Moment DCR of flexural beams in S-615 and S-914 prototype structures for DBE hazard level

and S-914 prototypes are 0.910 and 0.872, respectively, and 100% of the data are lower than 1 in this hazard level. Therefore, all members had an elastic behavior in DBE hazard level. Obviously, the link beams of the LC system have a proper design, and are able to control the behavior of members of MF system to remain elastic.

6 Conclusions

The parametric results of the present research, as the continuation and development of the design method presented in reference [14] are more comprehensive due to the use of LCF structures with different lateral relative stiffness between the LC and MF systems and clarify the applicability of the proposed design method for a wide range of structures. In the proposed design method of this paper, the requirements for the ductile beam in the MF system and also the determination of the distance between the displacement at the first yield in the link beam in LC system and the first yield in the flexural beam in MF system are presented.

There are three performance objectives in the design of ideal Linked Column Frame system. The force-based methods cannot guarantee to achieve the target performance objectives, and therefore, the performance-based methods should be applied. The design method proposed in this study for the linked column frame systems uses the performance-based plastic design (PBPD) for this purpose. This is an iterative and simple procedure to design the structure for the different performance objectives with adequate accuracy. By this method, in addition to achieving the performance objectives, the link beams have a proper design and protect the other structure members from yielding. For parametric assessment, the design examples for this method are 9 structure with 3, 6 or 9 stories and with 3, 4 or 5 number of bays, and their performances are evaluated by nonlinear static and nonlinear time-history dynamic analyses. For nonlinear dynamic analysis, two prototype structures are subjected to 66 different ground motion records in three different hazard levels. The analyses results show the simplicity, accuracy and efficiency of this method. According to parametric study in design, evaluation and analysis procedures, the following results are obtained:

1. The proposed method is simple and converges fast.
2. It is highly accurate with considering the interactions of LC and MF systems.
3. According to the parametric studies and nonlinear static analysis, all the link beam members yield before the MF members, and the yield mechanism is comparable with presumed mechanism.
4. Based on parametric studies, the designed structures with proposed design method with different lateral stiffness of MF and LC systems are achieved all three performance objectives properly.
5. In the designed prototypes with the proposed method for the earthquake with 50% probability of exceedance in 50 years (SLE), all the structure members remain elastic.
6. In the designed prototypes with the proposed method for the earthquake with 10% probability of exceedance in 50 years (DBE), only the link beams of LC system started to yield and all flexural beams of MF system remained elastic. Therefore, the link beam functions according to the structural fuse concept.
7. Based on parametric studies and as it was also shown earlier in reference [14] the displacements of the designed prototypes, under hazard levels of DBE and MCE are lower than the target displacements.
8. According to parametric studies, the proposed design method is well suited for a wide range of structures with linked column frame system.

References

[1] Aiken, I., Clark, P., Tajirian, F., Kasai, K., Kimura, I., Ko, E. "Unbonded braces in the United States - Design studies, large-scale testing, and the first building application". In: *Symposium of Passive Control Structure–2000, Tokyo Institute of Technology* (pp. 203–217), 2000.

[2] Saeki, E., Iwamatu, K., Wada, A. "Analytical study by finite element method and comparison with experiment results concerning buckling-restrained unbonded braces". *Journal of Structural and Construction Engineering*, 484, pp. 111–120. 1996. https://doi.org/10.3130/aijs.61.111_2

[3] Sabelli, R., Mahin, S., Chang, C. "Seismic demands on steel braced frame buildings with buckling-restrained braces". *Engineering Structures*, 25(5), pp. 655–666. 2003. https://doi.org/10.1016/S0141-0296(02)00175-X

[4] Iwata, M., Kato, T., Wada, A. "Buckling-restrained braces as hysteretic dampers". In: *Proceedings of the 3rd International Conference on Behavior of Steel Structures in Seismic Areas (STESSA 2000), Montreal, Canada* (pp. 33–38). 2000.

[5] Deierlein, G., Krawinkler, H., Ma, X., Eatherton, M., Hajjar, J., Takeuchi, T., Midorikawa, M. "Earthquake resilient steel braced frames with controlled rocking and energy dissipating fuses". *Steel Construction*, 4(3), pp. 171–175. 2011. 10.1002/stco.201110023

[6] Eatherton, M. R., Hajjar, J. F., Deierlein, G. G., Krawinkler, H., Billington, S., Ma, X. "Controlled rocking of steel-framed buildings with replaceable energy-dissipating fuses". In: *Proceedings of the 14th World Conference on Earthquake Engineering* (pp. 12–17). 2008.

[7] Pollino, M. "Seismic design for enhanced building performance using rocking steel braced frames". *Engineering Structures*, 83, pp. 129–139. 2015. 10.1016/j.engstruct.2014.11.005

[8] Dusicka, P., Iwai, R. "Development of Linked Column Frame System for Seismic Lateral Loads". In: *Structural Engineering Research Frontiers* (pp. 1–13). American Society of Civil Engineers. 2007.10.1061/40944(249)63

[9] Lopes, A. P., Dusicka, P., Berman, J. "Linked column frame steel system performance validation using hybrid simulation". In: *Proc. of Tenth US National Conference on Earthquake Engineering, Anchorage, Alaska*. 2014.

[10] Malakoutian, M., Berman, J. W., Dusicka, P. "Seismic response evaluation of the linked column frame system". *Earthquake Engineering & Structural Dynamics*, 42(6), pp. 795–814. 2013. 10.1002/eqe.2245

[11] Malakoutian, M., Berman, J. W., Dusicka, P., Lopes, A. "Quantification of Linked Column Frame Seismic Performance Factors for Use in Seismic Design". *Journal of Earthquake Engineering*, 20(4), pp. 535–558. 2016. 10.1080/13632469.2015.1104750

[12] Lee, S. S.-S., Goel, S. S. C., Chao, S. H. "Performance-based seismic design of steel moment frames using target drift and yield mechanism". *13th world conference on Earthquake*, (266). 2004. Retrieved from http://www.iitk.ac.in/nicee/wcee/article/13_266.pdf

[13] Goel, S. C., Chao, S., Leelataviwat, S., Lee, S. "Performance-Based Plastic Desig (PBPD) Method for Earthquake-Resistant Structures". In: *The 14 World Conference on Earthquake Engineering. Beijing, China*. 2008.

[14] Shoeibi, S., Kafi, M.A., Gholhaki, M. "New performance-based seismic design method for structures with structural fuse system". *Engineering Structures*, 132, pp. 745–760. 2017. 10.1016/j.engstruct.2016.12.002

[15] Mazzoni, S., McKenna, F., Scott, M. H., Fenves, G. L. "Open system for engineering simulation user-command-language manual, version 2.0, Pacific Earthquake Engineering Research Center". *University of California, Berkeley, Berkeley, CA*. 2009.

[16] Chao, S.-H., Goel, S. C., Lee, S.-S. "A Seismic Design Lateral Force Distribution Based on Inelastic State of Structures". *Earthquake Spectra*, 23(3), pp. 547–569. 2007. 10.1193/1.2753549

[17] Chao, S.-H., Goel, S. C. "Performance-based seismic design of eccentrically braced frames using target drift and yield mechanism as performance criteria". *Engineering Journal. American Institute of Steel Construction, Inc*, 43(3), pp. 173–200. 2006.

[18] Kharmale, S. B., Ghosh, S. "Performance-based plastic design of steel plate shear walls". *Journal of Constructional Steel Research*, 90, pp. 85–97. 2013. 10.1016/j.jcsr.2013.07.029

[19] Chao, S.-H., Bayat, M. R., Goel, S. C. "Performance-based plastic design of steel concentric braced frames for enhanced confidence level". In: *14th World conference on Earthquake Engineering, Beijing, China* (pp. 12–17). October 12–17, 2008.

[20] Dasgupta, P., Goel, S. C., Parra-montesinos, G., Tsai, K. C. "Performance-Based Seismic Design and Behavior of a Composite Buckling Restrained Braced Frame". *13th World Conference on Earthquake Engineering*, (497), pp. 153–164. 2004.

[21] Newmark, N. M., Hall, W. J. "Earthquake spectra and design". *Earth System Dynamics*, 1. 1982.

[22] ASCE 7–10. *Minimum Design Loads for Buildings and Other Structures*. Standards. American Society of Civil Engineers. 2010. 10.1061/9780784412916

[23] Krawinkler, H. *State of the art report on systems performance of steel moment frames subject to earthquake ground shaking. Rep. No. FEMA-355C, Federal Emergency Management Agency, Washington*, DC. SAC Joint Venture. 2000.

[24] AISC 341-10. "Seismic Provisions for Structural Steel Buildings,(ANSI/AISC 341-10)". American Institute of Steel Construction, Chicago, IL. 2010.

[25] BHRC-2800. *Iranian code of practice for seismic resistant design of buildings: Standard No. 2800* (4th ed.). Tehran: Road, Housing and Urban Denelopment Research Center. 2014.

[26] FEMA P695. *Quantification of building seismic performance factors*. Washington, D.C.: Technical Report P695, Applied Technology Council for the Federal Emergency Management Agency. 2009.

[27] Dusicka, P., Lewis, G. "Investigation of replaceable sacrificial steel links". In: *Proceedings of the 9th US National and 10th Canadian Conference on Earthquake Engineering* (Vol. 1659). 2010.

[28] Sumner, E. A., Murray, T. M. "Behavior of extended end-plate moment connections subject to cyclic loading". *Journal of Structural Engineering*, 128(4), pp. 501–508. 2002. 10.1061/(ASCE)0733-9445(2002)128:4(501)

[29] Liu, J., Astaneh-Asl, A. "Moment-rotation parameters for composite shear tab connections". *Journal of Structural Engineering*, 130(9), pp. 1371–1380. 2004. 10.1061/(ASCE)0733-9445(2004)130:9(1371)

[30] ASCE 41-13. *Seismic Evaluation and Retrofi t of Existing Buildings*. American Society of Civil Engineers. 2013.